



Electrical characterization of circulation weather types in Northern Spain based on atmospheric nanoparticles measurements: A pilot study

Pablo Fdez-Arroyabe^{a,*}, Ciro Luis Salcines Suárez^b, Ion-Andrei Nita^c, Pavlos Kassomenos^d, Elias Petrou^d, Ana Santurtún^e

^a University of Cantabria, Department of Geography and Planning, Geobiomet Research Group, Santander, Spain

^b University of Cantabria, Health and Safety Unit, Infrastructures Service, Santander, Spain

^c National Meteorological Administration, Alexandru Ioan Cuza University, Doctoral School of Geosciences, Iasi, Romania

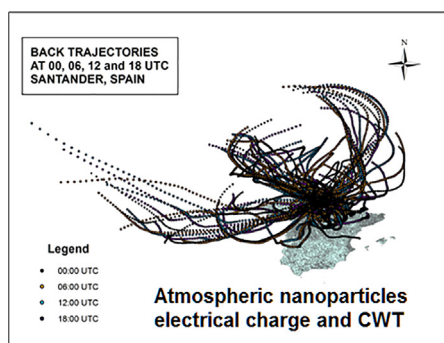
^d University of Ioannina, Department of Physics, Laboratory of Meteorology, GR-45110 Ioannina, Greece

^e University of Cantabria, Department of Physiology and Pharmacology, Geobiomet Research Group, Santander, Spain

HIGHLIGHTS

- Atmospheric nanoparticles can be used to characterize air masses electrically.
- Coarse nanoparticles are mainly negative up to 12 UTC and then turn to positive.
- The highest mean absolute charge of particles is linked to winds nearby Santander.

GRAPHICAL ABSTRACT



ARTICLE INFO

Article history:

Received 26 June 2019

Received in revised form 29 October 2019

Accepted 30 October 2019

Available online 20 November 2019

Editor: Snezana Dragovic

Keywords:

Nanoparticles
Electric charge
Weather type
Back trajectories

ABSTRACT

The electrical component of the atmosphere is a key element to understand bio-effects of atmospheric processes. In this paper an attempt was made to find possible interactions between air masses arriving in Santander, Northern Spain, and electrical properties of nanoparticles measured in this zone. A methodological approach is proposed to characterize electrically the predominant weather types in the study area. An electrical low pressure impactor device (ELPI[®]+) was used to measure atmospheric particles net charge and particle net charge distribution in real time in July 2018, among other parameters. Data from two specific channels [0.054–0.071 μm] and [2.5–3.0 μm] has been initially used. Atmospheric circulation was defined attending to two, subjective and objective, weather type classifications. Back trajectories of nanoparticles were also computed by the Hybrid Single-Particle Lagrangian Integrated Trajectory model. Results confirm that atmospheric nanoparticles charge varies according to their size. The highest mean absolute charge is associated with local circulation in Santander for both channels. The studied nanoparticles show a quicker reaction to weather conditions than microparticles. They also have a significant correlation with meteorological variables for 18 synoptic groups found, but humidity. Microparticles [2.5–3.0 μm] are negatively related with air humidity, mainly with S-SE circulation pattern.

© 2019 The Author(s). Published by Elsevier B.V. This is an open access article under the CC BY-NC-ND license (<http://creativecommons.org/licenses/by-nc-nd/4.0/>).

* Corresponding author.

E-mail addresses: fernandhp@unican.es (P. Fdez-Arroyabe), ciroluis.salcines@unican.es (C.L. Salcines Suárez), pkassom@uoi.gr (P. Kassomenos), ana.santurtun@unican.es (A. Santurtún).

1. 1. Introduction

Air pollution has become a global priority in terms of minimizing the impact of CO₂ on global warming due to climate change. Moreover, during the last decade several epidemiological and experimental studies have shown the relationship between high levels of pollutants, specifically particulate matter, and morbimortality (Kim et al., 2018; Sanyal et al., 2018), specially due to cardiovascular and respiratory diseases (Fdez-Arroyabe and Robau, 2017; Lelieveld et al., 2019; Royé et al., 2018).

Particles suspended in gases can be classified as microparticles or nanoparticles. Microparticles have diameters in the micrometre size range, while nanoparticles are smaller than 1 µm. Nanoparticles produce very slight light scattering, thus being practically invisible, and they follow the stream lines of their carrier gas, hence not impacting on obstacles at atmospheric gas pressure (Zhiqiang et al., 2000).

Nowadays, the social concern about the impact of aerial nanoparticles on the environment and on human health has risen significantly (Garcia-Mouton et al., 2019). However, very few nanoparticle measurements have been performed, which makes it difficult to study their effects.

The detection of atmospheric nanoparticles and the measurement of specific properties associated with them (such as concentration, size, distribution, electrical properties and chemical composition) are necessary (Scientific Committee on Emerging and Newly Identified Health Risks [SCENIHR], 2006). Some authors suggest that atmospheric nanoparticles and their electric field may play an important role in atmospheric processes and in heterogeneous chemical reactions that take place in the troposphere (He et al., 2019; Järvinen et al., 2017; Kubicki et al., 2016).

The concentration and size distribution of nanoparticles as a function of aerodynamic particle size in real-time can be measured by using an Electrical Low Pressure Impactor (ELPI[®]+). In an ELPI's cascade impactor, the sampled and unipolarly charged aerosol is classified into size fractions. Electrometers are then used to simultaneously measure the currents resulting from the collected charged particles from electrically insulated impactor stages. The nominal flow rate of the instrument is 10 L/min. In the original construction, the particle size range measured by the ELPI[®]+ ranges from 30 nm to 10 µm (Yli-Ojanperä et al., 2010). Marjamäki et al. (2002) extended the electrically measured size range down to 7 nm by adding a final (in the flow direction of the device) filter stage.

Synoptic scale meteorological patterns determine the conditions for the long-range transport of atmosphere particles, while also affecting the interaction among them (Santurtún et al., 2015). Climatologists have dealt with the topic of systematizing atmospheric circulation conditions by means of a catalog of weather types (WTs), which has led to the existence of several classification methods, both manual methods, such as those proposed by Lamb and Britain (1972) for the British Islands and semi-automatized techniques which allow for the analysis of large amounts of data in less time and effort (e.g., Esteban et al., 2006; Beck and Philipp, 2010).

The main hypothesis of this work is that atmospheric conditions and air mass types are associated with the electric charge of nanoparticles. Additionally, we posed that atmospheric electric charge in the city of Santander is associated with local winds circulations.

The aim of this study is to describe the electrical properties of the nanoparticles measured in the north of Spain and to analyse their relationship with subjective atmospheric dispersion models and weather types.

2. Materials and methods

The present work studies the concentration and size distribution of nanoparticles and their relationship with meteorological conditions in Santander, a northern coastland city of Spain which has a humid temperate oceanic climate, for nearly 1 month (from 4th to 31st July 2018). Secondly, it analyzes the association between nanoparticles features and subjective and objective weather types attending to intraday oscillations.

2.1. Data and instrumentation

Meteorological data has been obtained from the Spanish Agency of Meteorology (AEMET) at the weather station of Santander CMT, (Cod. 1111X), located at 52 m above mean sea level at coordinates 3.801 W, 43.490 N. Temporal resolution of datasets is 10 min and variables recorded are temperature (Celsius), wind speed (m/s), wind direction (degrees), direction of maximum wind speed (degrees), relative humidity (%) and atmospheric pressure (hPa).

Electrical charge of nanoparticles was registered with an ELPI[®]+ device (Fig. S1) that was lent to the Geobiomet research group from the University of Cantabria, in the experimental frame of the COST Action 15211 Electronet, by DEKATI Company. ELPI[®]+ is an electrical low pressure impactor that works with 14 channels (Dekati, 2019). The device recorded data at the roof of one of the buildings of the University of Cantabria (UC) (Geographic location at 3.803 W, 43.471 N) for almost one month (July 2018).

ELPI[®]+ was used to measure particle net charge and particle net charge size distribution in real-time. The measurements were conducted by switching the ELPI[®]+ charger off with 30–40 s periods of time (at least 20 s recommended for the charger voltage to stabilize). In this setup, both positive and negatives charge levels are obtained and were measured in the different channels or impactor stages, giving the particle size fractions. The values are in femto Amperes (fA).

The collected charge nanoparticles data were debugged during most of July 2018 in 14 different classes according to the dimensions of nanoparticles from 6 nm to 10.000 nm. Values from channels 4 and 12 have been used for this study. They correspond to the dimensions of [0.054–0.071 µm] and [2.5–3.0 PM] respectively. Channel 4, henceforth Ch 0.072, is the most reliable in relation to the theoretical definition of nanomaterials [1–100 nm] (Lidén, 2011) having less rebound in the collection of samples while channel 12, henceforth Ch 3.037, corresponds to the lowest standard measurement of atmospheric particulate matter (PM 2.5).

Fig. 1 presents the nominal impactor specifications for the two used channels, taken from the ELPI[®]+ manual. Exact values for each specific ELPI[®]+ unit can be found in the calibration data sheet of the DEKATI[®] ELPI[®]+ User Manual version 1.55. Stage refers to channels; D50% [µm] is the diameter limit for each stage; and Di [µm] refers to Stokes diameter.

The nanoparticles charge data were collected every second and integrated to 10 min time intervals mean values. Extreme values were deleted using 10th and 90th percentiles for each considered channel and clean data were integrated into 1 h, 6 h and daily scales.

2.2. Trajectory modelling

In order to describe the airflow reaching Santander, Spain (3.822 W, 43.426 N) at 500 m arrival height above mean sea level (AMSL), four hours per day (00, 06, 12, 18 UTC), three-day kinematic three-dimensional back trajectories, with time intervals

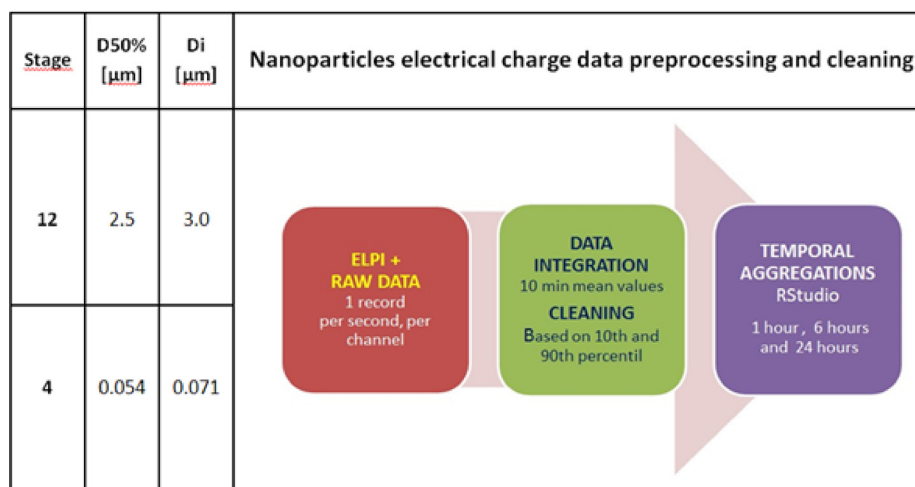


Fig. 1. Nanoparticles electrical charge data preprocessing and cleaning by channel.

between consecutive trajectory points equal to 1 h, were calculated.

These back trajectories were computed by the Hybrid Single-Particle Lagrangian Integrated Trajectory (HYSPLIT, release 4.7) model (Draxler and Hess, 1998; Draxler and Rolph, 2003). National Oceanic and Atmospheric Administration (NOAA) global reanalysis meteorological data were used (<http://ready.arl.noaa.gov/HYSPLIT.php>). These data were produced by the National Center for Environmental Prediction (NCEP) Global Data Assimilation System (Kanamitsu, 2002) which uses the spectral Medium-Range Forecast Model (MRF) for the weather forecast. The horizontal resolution of the trajectories matched the resolution ($2.5 \text{ km} \times 2.5 \text{ km}$) of the reanalysis data. All in all 40 vertical levels were used.

Three-dimensional trajectories were selected because they are more accurate than any other type of trajectories, including isentropic ones (Martin et al., 1990; Stohl, 1998). The length of back trajectories depends on the distances between sources and destinations zones and the paths that the air mass follows. The degree of accuracy for any single trajectory is generally unknown unless the trajectories are analysed as part of a tracer study.

2.2.1. Cluster analysis of atmospheric back trajectories

The first attempts of classifications were manual (Lamb, 1972, for the British Isles; Hess and Brezowsky, 1977, for central Europe) and were highly subjective since they depended on the investigator's experience, skills, and knowledge of the local and regional meteorological conditions. In order to reduce the subjectivity of these classifications the statistical technique of Principal Component Analysis (PCA) was introduced in early 90's. The cluster analysis (CA) was the crucial step to jump from subjectivity to "objectivity". Kalkstein et al. (2002) compared three clustering procedures in order to select the most suitable synoptic classification scheme. Similar research results using the same techniques were published by Moody and Samson (1989), Moody and Galloway (1988), Esteban et al. (2006), Philipp (2009), Markou and Kassomenos (2010), Remoundaki et al. (2013) among others.

Cluster analysis (CA) is a statistical technique used to group the observations into clusters such that each of them is as homogeneous as possible with respect to the clustering variables (Sharma, 1996). This multivariate statistical method was for the first time applied to atmospheric circulations by Moody and Samson (1989) and Moody and Galloway (1988). Since then, many researchers (Dorling et al., 1992; Dorling and Davies, 1995; Brankov et al., 1998; Cape et al., 2000; Jorba et al., 2004; Eneroth et al., 2003; Abdulmogith and Harrison, 2014; Borge et al., 2007;

Markou and Kassomenos, 2010; Kassomenos et al., 2007) had applied cluster analysis techniques to categorize back trajectories.

In this work, we used the K-means hierarchical cluster analysis using SPSS statistical package (Version 20). In order to define the number of clusters we adopted the formula proposed by McGregor, 1993, Number of Clusters = $1 + 3.3 \log N$ where N is the number of cases. We found five clusters namely SW, W, NE, NW and Local. From the clusters found two of them, e.g. W and NE, are associated with longer trajectory paths while the rest three are associated with shorter trajectory paths.

2.3. Weather types

Additionally, an objective classification method called GrossWetterTypen – GWT is used to derive circulation weather types over Santander. It is based on threshold criteria where each weather type is constructed using specific coefficients to define its zonality, meridionality or vorticity. These criteria are determined as spatial correlation between the daily Mean Sea Level Pressure (MSLP) and so-called idealized prototypical patterns representing the isobars in terms of direction (i.e. W-E or N-S) or cyclonicity over a spatial domain. GWT was constructed using MSLP from ECMWF ERA-Interim (Dee et al., 2011) at every 6 h each day over a spatial territory defined as a polygon centered over Santander (~2000 km to each margin). The classification was created using the software named "cost733class" (Philipp et al., 2014) created at the COST Action 733. The period considered to define the GrossWetter Typen – GWT was 1979–2018.

The 18 weather types were grouped into nine major categories for analytical purposes, in respect with the prevalent air advection direction and their (anti)-cyclonicity properties. The output of the proposed GWT aggregation is presented in Table 2.

A correlations analysis for each channel upon multiple meteorological variables for data aggregated at every 10 min was calculated. The confidence level was set at 90% (two-tailed test). Five synoptic groups are considered in this case (E-SEc, S-SEa, S-SWa, W-NWa, High Local) attending to their frequency (more than 80% of the total) and their similarity to the mean back trajectories previously studied.

3. Results

3.1. Atmospheric variables and nanoparticles electrical charge

Fig. 2 shows the time series (ten minutes) of the electrical charge (fA) of the studied stages (Ch. 0.072, left top), (Ch. 3.037,

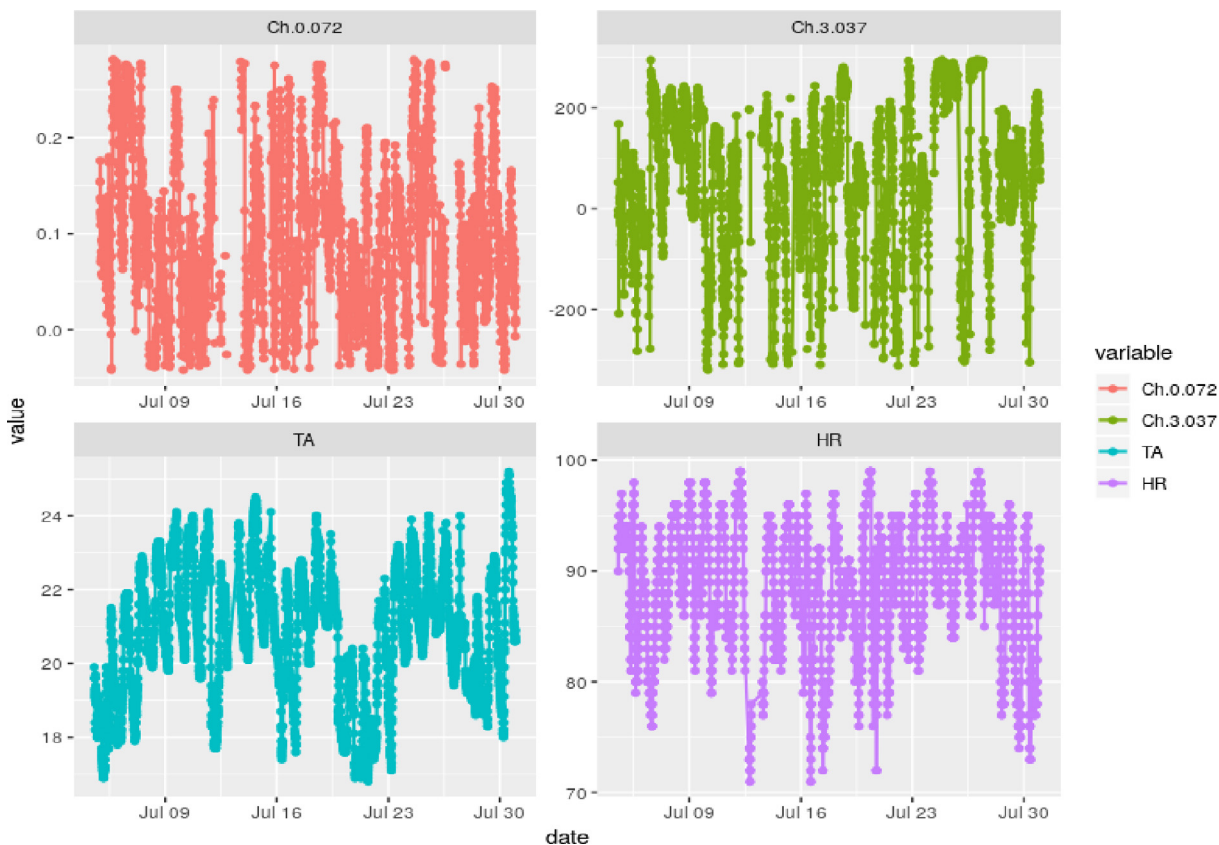


Fig. 2. Ten minutes mean of the electrical charge for Ch. 0.072 (left top) and Ch. 3.037 (right top) and their corresponding air temperature (bottom left) and relative humidity values (bottom right) in Santander.

right top) and the corresponding values of air temperature (bottom left) and relative humidity (bottom right) in Santander. There is a significant statistical correlation ($CC = 0.49$; $p < 0.05$) between records of both channels. Channel 4 data shows a negative correlation with air humidity ($CC = -0.32$; $p < 0.05$) and a small but significant correlation with temperature values and wind. Channel 12 is only correlated with temperature. Atmospheric pressure is not statistically related with the electrical charge of nanoparticles at this specific temporal scale.

Six hours (left) and daily (right) mean values of nanoparticles electrical charge (fA) are represented for both channels in Fig. 3. The temporal distribution of mean charge every six hours is correlated with the hour of the day in both channels ($CC = 0.40$; $p < 0.05$).

At the six hours temporal scale, positive mean values of charge were predominant in the Ch. 0.072 being the highest charges recorded in days 13, 6, 5, 18, 24 and 25. Only days 7 and 22 recorded negative charge mean values in this channel. On contrast, values in Ch. 3.037 are well distributed between positive and negative charge values. Daily mean values of charge for Ch. 0.072 present a slightly negative trend during July while it is slightly positive for Ch. 3.037 values.

3.2. Atmospheric back trajectories and nanoparticles

From the analysis of the computed back trajectories and the classification of them using K-means cluster analysis four times per day (0,6,12,18 UTC) we found 5 clusters, describing the air masses coming from SW, W, NE, NW, in Santander while in addition an extra cluster describes the air masses moving around

Santander and could be characterized as “Local”. From the clusters found only W and NE are long while the rest are short.

The mean trajectories per air mass type were computed at 500 m; Fig. 4 (a-d) shows the mean trajectories of the five clusters per 6 h. The air masses coming from W and NE, passing over Atlantic Ocean and Europe mainland respectively, have longer paths while the rest ones especially local have shorter paths.

It must be noted that “Local” circulations are the most frequent with percentage of occurrence ranging between 42.9% and 25% (see Table 3 below). In this case, the air masses are moving around the area of Santander and have enough time to absorb the surface characteristics (marine or land) of the area. It is the warmest category since the temperature (500 m above ground) in the arrival point was between 290.3 and 293.5 K. This category combines with the smallest values of Relative Humidity (RH) (69.1–78.7%). For all the hours, the total rainfall during the route is by far the highest, ranging between 9 and 12 mm.

The second most frequent category is NW with percentage of occurrence ranging between 28.6 and 25%. It describes air masses coming from the nearby Cantabrian Sea and in most of the cases has short routes absorbing the main surface characteristics of the area passing above. This category is one, not surprising, of the most humid since the RH ranges between 85.2 and 82.7% and coldest since temperature is ranging between 287.3 and 289.5 K. The total rainfall during the route ranged between 2.2 and 3.1 mm.

The third most frequent category is SW with percentage of occurrence between 17.9 and 10.7%. It describes air masses arriving in Santander from SW. These air masses originate over the west coasts of Iberian Peninsula and in most of the cases are passing over the Iberian mainland before their arrival to Santander. Their route could be characterized as short (in most of the cases) so they



Fig. 3. Standardized values of six hours and daily mean nanoparticles electrical charge (fA) for channel Ch. 0.072 and Ch. 3.037 in Santander, Northern Spain.

probably absorb some of the surface characteristics passing over. Their temperature at the arrival point ranges between 288 and 293.1°K and the relative humidity 67.6–84.5%. The total rainfall during the route was 0–6.6 mm.

NE category describes air masses coming from the mainland Europe (usually from France and central Europe). They are fast moving air masses with long routes, so they cannot absorb the surface characteristics of the area they passing. The percentage of occurrence of this category is 14.3–10.7%, with temperatures in the arriving point ranging between 290.2 and 292.6 K and Relative Humidity 70.3–75.3%. The total rainfall during the route was between 0.2 and 5.2 mm.

Finally, W category describes fast moving air masses with very long routes originated in the middle Atlantic Ocean. Occurrence of these air masses ranges between 7.1 and 25% depending of the hour of the day. Their temperature ranged between 298.3 and 292.3 K and relative humidity 70.8–75.9%. The total rainfall through the route was 0.2–10.7 mm depending from the hour of the day.

Table 1 shows the main meteorological characteristics per back trajectory class and time (00, 06, 12, 18): Frequency expressed in percentage of occurrence (%); Temperature (K) at 500 m above ground; Atmospheric Pressure (hPa) at 500 m above ground; Rain (mm) during the whole trajectory route (72 h); Relative Humidity (%) at 500 m above ground.

In order to correlate air mass types with the electrical properties of the particles measured in Santander we took under consideration only two channels of the available 14 channels in which we have recorded electrical data. We have chosen one band with nanoparticles with diameter 0.072 μm (like 72 nm) and one band with almost PM_{2.5} particles (3.037 μm).

The recorded electrical charge values of PM_{3.037} μm and PM₇₂ nm integrated per 6 h were studied (Figs. S2 and S3) Starting from

low values charge at 6.00 UTC in all the air mass types, there is a direct effect of the solar radiation and the increase of the nanoparticles charge. For almost all the air mass types, it was found that at 12.00 UTC the nanoparticles have the higher absolute electric charge, following by the nanoparticles collected at 18.00 UTC. Dispersion of nanoparticles charge values was $\sigma = 0.057$ at 00 UTC and $\sigma = 0.051$ at 6 UTC, being maximum dispersion found at 12 UTC with $\sigma = 0.073$.

This means that the intensity of solar radiation entails an increase of electric charge in the sub-100 nm size range and maintains for several hours. This could be a sign of new particle formation (Kerminen et al., 2018). It is remarkable that Local circulations are combined with nanoparticles with the higher absolute electric charge, following by NW type. High values are also found with SW type while for NE and W types the nanoparticles have the lowest absolute electric charge (Fig. 5).

On the contrary to nanoparticles, no significant differences were found in electric charge of the particles with diameter 3.037 μm concerning the hours of the day. Dispersion of values in this case are concentrated at 0 and 6 UTC respectively ($\sigma = 134.5$ and $\sigma = 122.4$). Much lower dispersion of values is found at noon ($\sigma = 100.9$) and at 18 UTC ($\sigma = 101.4$).

Local circulations again present the higher absolute electric charge independently of the hour of the day following by NE type. Roughness of the city surface (buildings and topography) may introduce a wind friction factor to explain these high values but this cannot be proved in this study. High values were also found for SW type while lower values were associated with NW and W types (Fig. 6). Salt particles coming from the sea can also play a key role in the electrical charge of nanoparticles.

Since the effect of negative/positive charge to the human health is different, we tried to separate mean values of negative and positive charge. We found that with the exception of 00:00 UTC the

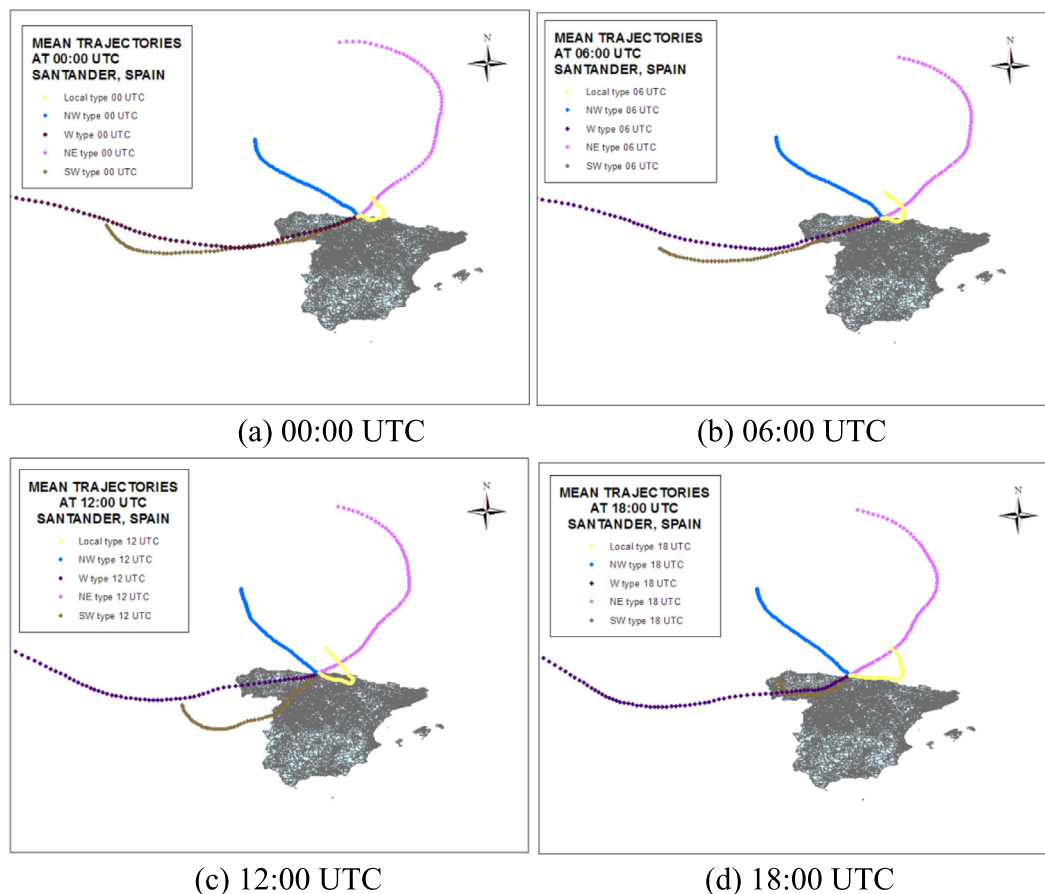


Fig. 4. Mean trajectories of the five air mass weather types arriving in Santander at 500 m for (a) 00:00, (b) 06:00, (c) 12:00, (d) 18:00 UTC.

Table 1
The main meteorological characteristics per back trajectory class and time.

	(%)	T (K)	P (hPa)	Rain (mm)	RH (%)	(%)	T (K)	P (hPa)	Rain (mm)	RH (%)
00:00 UTC						06:00 UTC				
SW	17.9	289.8	906.3	1.9	81.1	10.7	288.0	905.8	2.3	84.5
NE	10.7	290.6	908.4	0.2	74.5	14.3	290.2	908.3	3.2	75.3
W	7.1	291.1	910.5	6.3	70.8	7.1	289.7	905.7	2.2	75.9
NW	28.6	288.4	908.7	3.0	84.6	25.0	287.3	908.1	2.2	85.2
Local	35.7	292.1	907.0	9.2	78.7	42.9	290.3	906.1	8.2	78.7
12:00 UTC						18:00 UTC				
SW	10.7	289.7	906.9	6.6	80.7	10.7	293.1	906.3	0.0	67.6
NE	14.3	290.9	908.9	2.2	74.6	14.3	292.6	908.2	5.2	70.3
W	10.7	289.3	906.4	0.2	72.2	25.0	292.3	906.4	10.7	74.2
NW	28.6	288.0	908.0	1.4	84.1	25.0	289.5	908.0	3.1	82.7
Local	35.7	291.4	907.2	8.5	74.1	25.0	293.5	906.9	12.3	69.1

nanoparticles have positive charge while for 3.037 μm we found that the electric charge was mainly negative during 0 and 6 UTC trajectories. For these reasons we present Fig. 7(a–c) in which the negative/positive mean values per category and time were shown.

3.3. Electrical properties of GrossWetterTypen classification

For a better consistency, a second objective classification, the GrossWetter Typen (GWT) classification, was also computed and 18 weather type classes were initially defined for the study area (Fig. S4).

Aggregated GWT categories frequency and description are presented in Table 2. The group of S-SE anticyclonic is the most

frequent one (24.8%), follow by high local winds (17.3%) and S-SW anticyclonic type (16.8%).

For the period 1979–2018, circulation types H and Sa were the most frequent ones. On contrast, types Wc and SWc happened relatively few times (Fig. S5) in the study area. Attending the month of July only, type H is the most frequent one follow by types Wa and NWA. These two types have been more frequent in the study period (with almost 50% of presence on July) than they usually are.

Channels values are analysed attending to the cyclonic and anticyclonic weather types (Fig. S6). The electrical properties follow the same pattern for both cyclonic and anticyclonic groups. The density bins are higher for the anticyclonic groups due to the higher frequency of these weather types in July 2018 (around

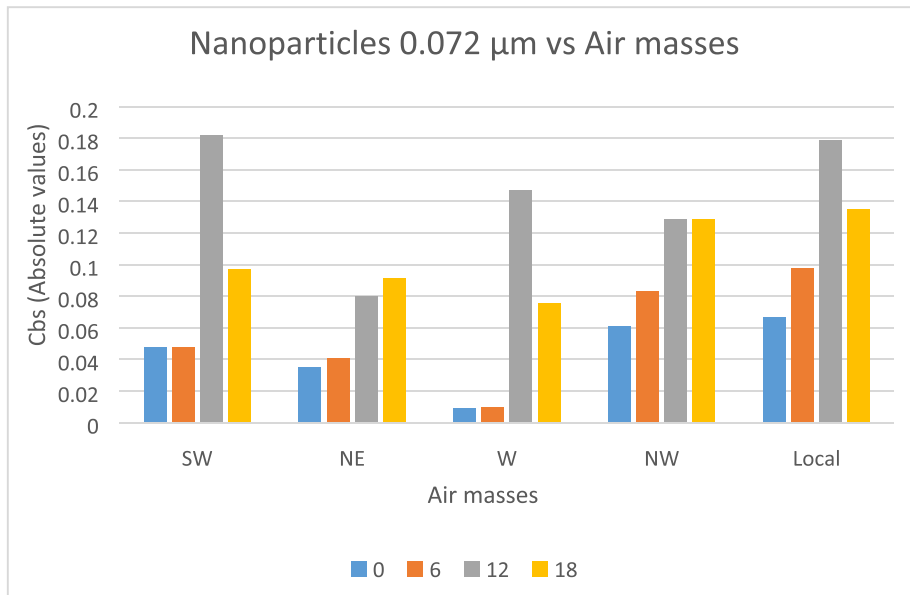


Fig. 5. Air mass types during July 2018 and mean absolute electric charge in 0.072 μm measured in Santander.

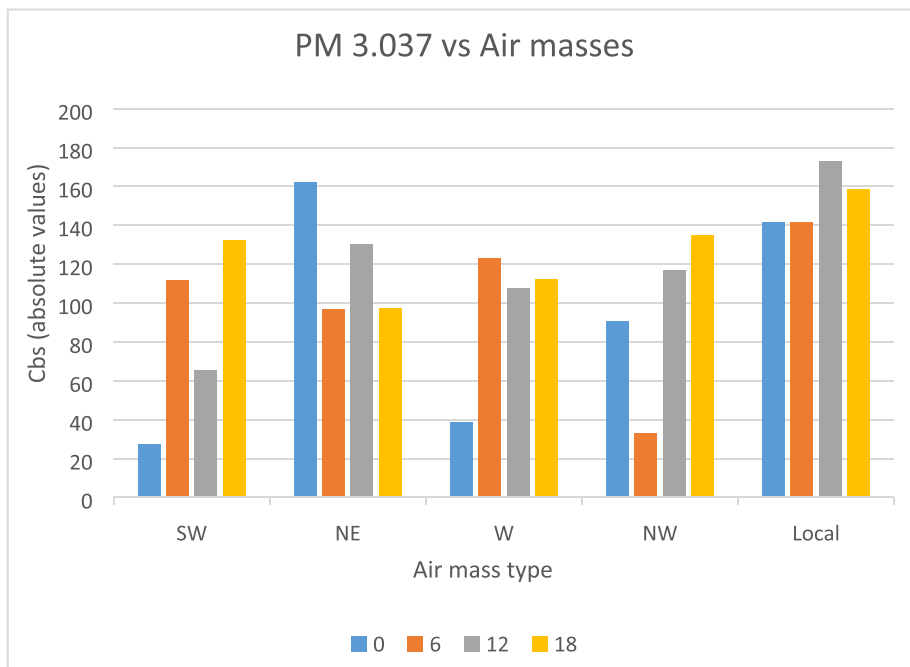


Fig. 6. Air mass types during July 2018 and mean absolute electric charge in PM 3.037 μm measured in Santander.

80% in total). For channel 0.072, the highest value is 0,144 fA recorded during the residence of a northerly anticyclonic (Na) weather type, while channel 3.037 records the greatest intensity also during the residence of an anticyclonic type (Centre High – H) with 173.82 fA, although the relative frequency for Na in July 2018 was around 1% compared with the 12.5% for H.

Lastly, we examined the links between the two studied channels and meteorological parameters in Santander adjacent to the synoptic groups that occurred in July 2018. Each synoptic group imprints a different pattern upon temperature or humidity content in the troposphere, which can affect the nanoparticles electrical charge.

We examined the Pearson correlations for each channel upon multiple meteorological variables for data aggregated at every 10 min. The confidence level was set at 95% (on a two-tailed test) meaning 2.5% to each side of distribution. Five synoptic groups are considered in this case (E-SEc, S-SEa, S-SWa, W-NWa, High Local) attending to their frequency (more than 80% of the total) and their similarity to the mean back trajectories previously studied. The variability between synoptic groups can be seen in Fig. 8. Since each group comprise multiple synoptic types, we put altogether the channels and meteorological data specific for the days when the synoptic types in every group occurred and calculated the correlation values

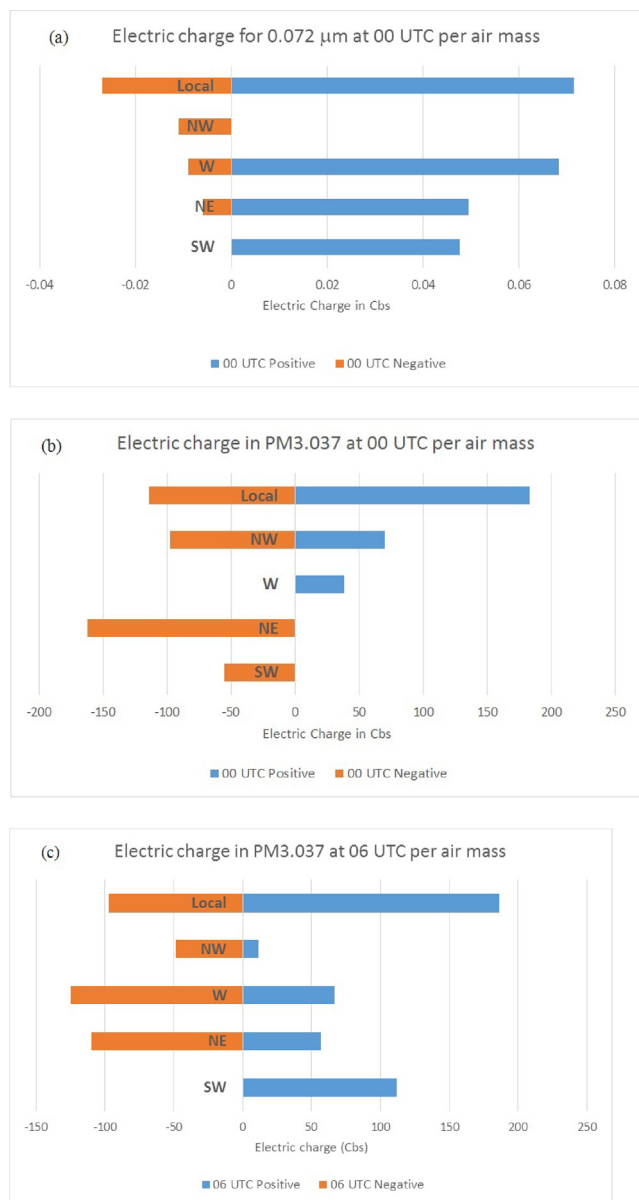


Fig. 7. Positive/negative mean electric charge for (a) nanoparticles at 00 UTC, (b) PM 3.037 at 00 UTC, (c) PM 3.037 at 06 UTC.

Generally, channel 0.072 has a significant correlation for all the synoptic groups with all the meteorological variables but humidity. On the other side, channel 3.037 is in good relation with humidity (negative correlation) during the residence of S-SEa synoptic group, possibly due to the advection of the drier air masses from the centre of Spain. Also, worth to mention here is the significant positive relation between all the channels and wind speed.

A statistical synthesis of the electrical properties of the particles in both channels per GWT is shown in Table 3. In the Ch 0.072 µm, there are specific situations of negative charge represented by their minimum values in the S-SWa and W-NWa types. However, the positive charge predominates for all circulation types. The coefficient of variation of charge in the High Local type doubles the values of the other circulation types. This confirms the singularity of the atmospheric electric charge in an urban environment such as Santander. This fact remains in the analysis of the Ch PM 3.037. It can be suggested the presence of a phenomenon of Urban Electric Island (UEI) where the characteristics of the urban

Table 2
Frequency and description of the aggregated GrossWetter Typen categories.

	%	Types	Description
1st	7.8	T1 – N cyclonic (Nc) T2 – NW cyclonic (NWc) T3 – NE cyclonic (NEc)	North Cyclonic
2nd	10.4	T4 – E cyclonic (Ec) T5 – SE cyclonic (SEc) T6 – S cyclonic (Sc)	E-SE Cyclonic
3rd	3.2	T7 – SW cyclonic (SWc) T8 – W anticyclonic (Wc)	W-SW Cyclonic
4th	24.8	T9 – South anticyclonic (Sa) T10 – SE anticyclonic (SEa)	S-SE Anticyclonic
5th	16.8	T11 – SW anticyclonic (SWa) T12 – W anticyclonic (Wa)	S-SW Anticyclonic
6th	11.2	T13 – NW anticyclonic (NWa) T14 – N anticyclonic (Na)	W-NW Anticyclonic
7th	5	T15 – NE anticyclonic (NEa) T16 – E anticyclonic (Ea)	N-NE Anticyclonic
8th	3.3	T17 – Central Low (L)	Central low-strong winds
9th	17.3	T18 – Central High (H)	High local winds

environment seem to alter the electrical properties of the nano and micro atmospheric particles in Santander.

The E-SEc type, being the least frequent, is the most singular in Ch PM 3.037 since it is the only one that maintains an average value of negative charge which it is not frequent in July in the study area.

4. Discussion

Our study has two main strengths. On the one hand, this is to the best of our knowledge the first work that characterizes the electrical charge of nanoparticles and its relationship with meteorological variables while considering intra-daily changes. On the other hand, it studies the association between weather types and nanoparticles, which could be the first step for formulating alert protocols depending on forecast atmospheric circulation patterns.

Recently, Garcia-Mouton et al. (2019) stated that the need for further information about the risks associated with the production and use of nanoparticles had led to the creation of different scientific disciplines, such as nanotoxicology (Garcia-Mouton et al., 2019). During the last few years, the knowledge about nanoparticles from different fields, such as chemistry (Kulmala et al., 2014), biology (Kumar et al., 2019), medicine (Hidalgo et al., 2017; Li et al., 2016), or physics (Sanderson et al., 2014), has grown significantly. However, the study of nanoparticles from a climatic perspective is still in its early stages.

Our results found that atmospheric conditions affect the capacity of nanoparticles for gaining or losing electric charge, and that the effects of atmospheric variability on nanoparticle charge happen faster than in microparticles. Furthermore, this relationship suggests that Weather Types could have an effect on the electric charge of nanoparticles: in Santander, the highest average absolute charge was found under local circulations (both for nanoparticles and PM3), doubling the values of the other circulation types. Local circulations are the most frequent and warmest category. We pose that, under those patterns, in which air masses are moving around the city, the surface characteristics of the area may affect nanoparticles for a longer time, and a phenomenon of Urban Electric Island (UEI) might appear. On the other hand, the proximity of Santander to the sea and the presence of marine aerosols can also be explanatory factors for this peculiar behaviour of the electric charge of atmospheric particles.

In a study which analyzed data from Santander, whose objective was to evaluate the relationship between Particulate Matter levels and admissions due to Chronic Obstructive

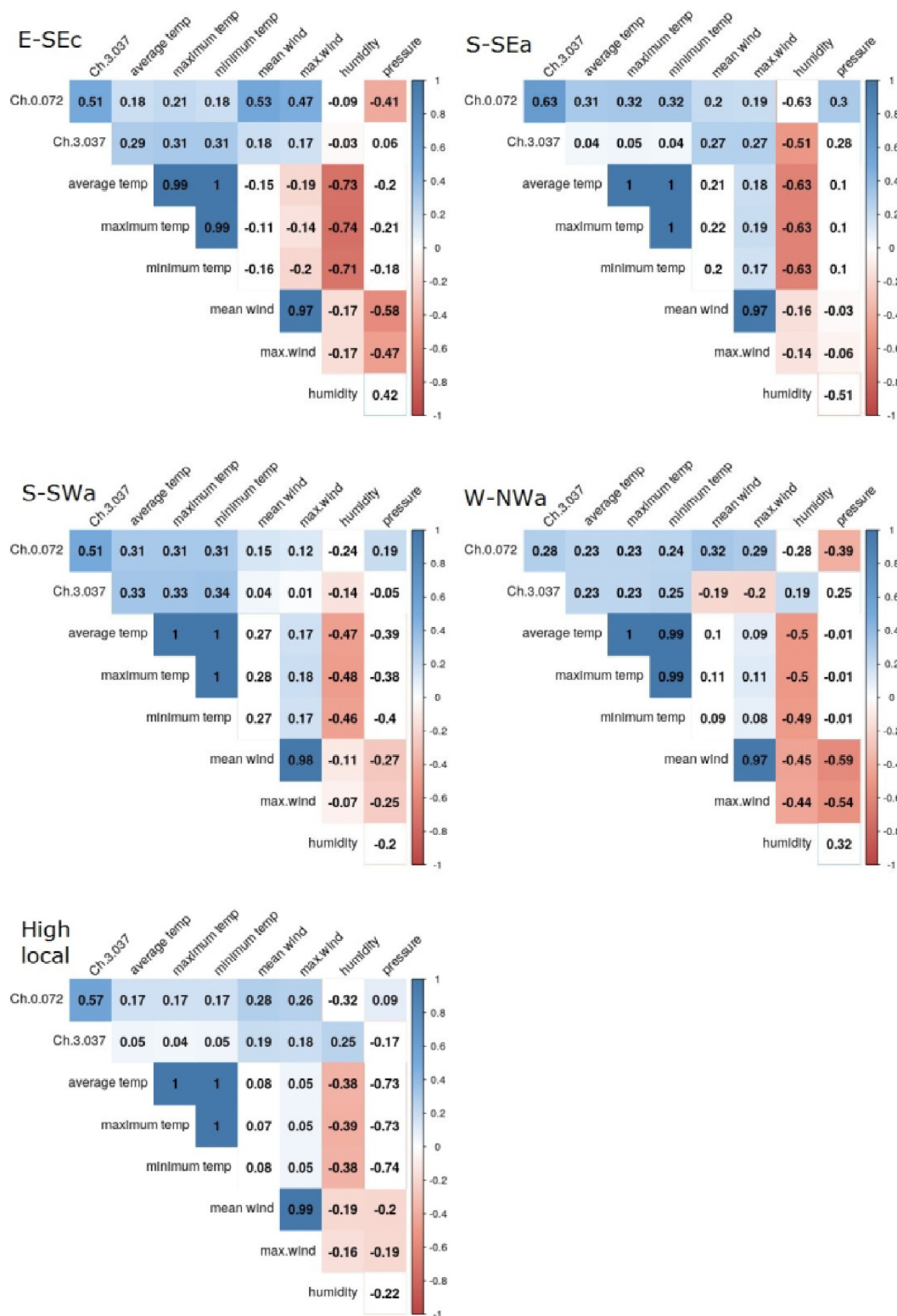


Fig. 8. Correlations between nanoparticles electrical charge and meteorological variables for each synoptic group (a) E-SEc, (b) S-SEa, (c) S-SWa, (d) W-NWa, (e) High local type.

Pulmonary Disease depending on the origin of the air masses (by using clustering isobaric trajectories), it was concluded that when the air masses were moving around the area of Santander, the effect on respiratory health was intensified (Santurtún et al., 2017). Although the authors hypothesized that the chemical com-

position of the particles might be the main factor behind this relationship, in view of our results the electric charge could also had played a role.

The main limitation of this study is the short period for which nanoparticle charge measurements were available (our group

Table 3
Summary of electrical properties by circulation type groups based on 6 h mean data from in Ch 0.072 μm and Ch PM 3.037.

Group Type	Frequency	Min	Max	Mean	Sum	SD
Ch 0.072 μm						
E-SEc	9	0.01	0.13	0.05	0.49	0.04
High Local	14	0.04	0.25	0.14	1.91	0.07
S-SEa	20	0.00	0.20	0.07	1.42	0.06
S-SWa	40	-0.01	0.25	0.08	3.21	0.07
W-NWa	25	-0.03	0.28	0.10	2.43	0.09
Ch PM 3.037						
E-SEc	9	-158.98	118.45	-21.49	-193.38	108.63
High Local	14	-116.39	272.03	129.97	1819.61	126.45
S-SEa	20	-218.06	290.47	45.00	900.07	143.02
S-SWa	40	-199.64	273.63	11.34	453.42	112.56
W-NWa	25	-214.03	262.33	87.17	2179.23	118.20

could only use the ELPI[®]+ device for 1 month). We intend to analyze a longer period, as well as study the potential seasonal effects on the electric charge of nanoparticles, in the near future.

5. Conclusions

In this paper an attempt was made to find possible interactions between air masses arriving in Santander, Northern Spain, and electrical properties of nanoparticles measured in Santander. It has been found that atmospheric nanoparticles charge can be used as a parameter to characterize weather type air masses electrically in the near future.

The analysis of the nanoparticles has revealed that air mass type could affect the electric charge of nanoparticles measured in the area. Specifically, coarse nanoparticles are mainly negative in charge up to 12 UTC and then turn to positive. Fine nanoparticles' charge is independent from the hour of the day and positive. Short moving air masses presented high values of electric charge.

The highest mean absolute charge is associated with local circulations in Santander (both for nanoparticles and PM₃). During the morning hours both bands are associated with significant number of negatively charged ions. 72 mean values nanoparticle show a faster reaction to weather conditions in its range than PM 2.5.

Moreover, the intensity of solar radiation entails an increase of electric charge in the sub-100 nm which maintains for several hours.

Atmospheric conditions affect nanoparticles ability to obtain or lose charge. The effects of atmospheric variability on nanoparticles charge take place quicker than in the microparticles in the studied channels.

Declaration of Competing Interest

The authors declare that they have no known competing financial interests or personal relationships that could have appeared to influence the work reported in this paper.

Acknowledgements

Authors would like to thank Dekati Ltd. for providing the instrument used in this study through the company SOLMA Environmental Solutions SLU.

Authors would like to thank NOAA Air researches Laboratory (ARL) for the provision of FNL-HYSPLIT data, the Hysplit transport and dispersion Model, and, the READY web site used in this publication.

Also authors acknowledge Cost Action 15211, Atmospheric Electricity Network: coupling with the Earth System, climate and biological systems, for funding a STSM of Prof. P. Kassomenos at

the Geobiomet research group at the University of Cantabria, Santander.

Authors would like to thank to support from the Spanish National Research Agency – Project CSO2016-75154-R and the European Funds for Regional Development (FEDER).

Appendix A. Supplementary data

Supplementary data to this article can be found online at <https://doi.org/10.1016/j.scitotenv.2019.135320>.

References

- Abdulmoghith, S., Harrison, R.M., 2014. The use of trajectory cluster analysis to examine the long-range transport of secondary inorganic aerosol in the UK. *School of Geography, Earth & Environmental Sciences The University of Birmingham. Atmos. Environ.* 39 (35), 1–21.
- Beck, C., Philipp, A., 2010. Evaluation and comparison of circulation type classifications for the European domain. *Phys. Chem. Earth Parts A B C* 37 (9e12), 374–387. <https://doi.org/10.1016/j.pce.2010.01.001>.
- Borge, R., Lumbrellas, J., Vardoulakis, S., Kassomenos, P., Rodríguez, E., 2007. Analysis of long-range transport influences on urban PM₁₀ using two-stage atmospheric trajectory clusters. *Atmos. Environ.* 41 (21), 4434–4450. <https://doi.org/10.1016/j.atmosenv.2007.01.053>.
- Brankov, E., Rao, S.T., Porter, P.S., 1998. A trajectory-clustering-correlation methodology for examining the long-range transport of air pollutants. *Atmos. Environ.* 32 (9), 1525–1534. [https://doi.org/10.1016/S1352-2310\(97\)00388-9](https://doi.org/10.1016/S1352-2310(97)00388-9).
- Cape, J.N., Methven, J., Hudson, L.E., 2000. The use of trajectory cluster analysis to interpret trace gas measurements at Mace Head, Ireland. *Atmos. Environ.* 34 (22), 3651–3663. [https://doi.org/10.1016/S1352-2310\(00\)00098-4](https://doi.org/10.1016/S1352-2310(00)00098-4).
- Dorling, S.R., Davies, T.D., 1995. Extending cluster analysis-synoptic meteorology links to characterise chemical climates at six northwest European monitoring stations. *Atmos. Environ.* 29 (2), 145–167. [https://doi.org/10.1016/1352-2310\(94\)00251-F](https://doi.org/10.1016/1352-2310(94)00251-F).
- Dorling, S.R., Davies, T.D., Pierce, C.E., 1992. Cluster analysis: a technique for estimating the synoptic meteorological controls on air and precipitation. *Chem.-Method Appl.* 26A (14), 2575–2581. Retrieved from Biostatistics.
- Draxler, R.R., Rolph, G.D., 2003. HYSPLIT (HYbrid Single-Particle Lagrangian Integrated Trajectory) Model access via NOAA ARL READY Website (<http://www.arl.noaa.gov/ready/hysplit4.html>). NOAA Air Resources Laboratory, Silver Spring, MD. Md.
- Draxler, R.R., Hess, G.D., 1998. An overview of the HYSPLIT_4 modelling system for trajectories, dispersion, and deposition. *Aust. Meteorol. Mag.* 47 (4), 295–308.
- Eneroth, K., Kjellström, E., Holmén, K., 2003. A trajectory climatology for Svalbard: investigating how atmospheric flow patterns influence observed tracer concentrations. *Phys. Chem. Earth.* 28 (28–32), 1191–1203. <https://doi.org/10.1016/j.pce.2003.08.051>.
- Esteban, P., Martín-Vide, J., Mases, M., 2006. Daily atmospheric circulation catalogue for Western Europe using multivariate techniques. *Int. J. Climatol.* 26 (11), 1501–1515.
- Fdez-Arroyabe, P., Robau, D.T., 2017. Past, present and future of the climate and human health commission. *Int. J. Biometeorol.* 61, 115–125. <https://doi.org/10.1007/s00484-017-1413-2>.
- García-Mouton, C., Hidalgo, A., Cruz, A., Pérez-Gil, J., 2019. The Lord of the Lungs: the essential role of pulmonary surfactant upon inhalation of nanoparticles. *Eur. J. Pharm. Biopharm.* <https://doi.org/10.1016/j.ejpb.2019.09.020>.
- He, Y., Gu, Z., Lu, W., Zhang, L., Okuda, T., Fujioka, K., Luo, H., Wah, Yu.C., 2019. Atmospheric humidity and particle charging state on agglomeration of aerosol particles. *Atmos. Environ.* 197, 141–149. <https://doi.org/10.1016/j.atmosenv.2018.10.035>.

- Hess, P., Brezowsky, H., 1977. Katalog der Grosswetterlagen Europas 1881–1976. 3. verbesserte und ergänzte Aufl. Berichte Des Deutschen Wetterdienstes, 113, 68.
- Hidalgo, A., Cruz, A., Pérez-Gil, J., 2017. Pulmonary surfactant and nanocarriers: Toxicity versus combined nanomedical applications. *Biochim. Biophys. Acta Biomembr.* 1859 (9 Pt B), 1740–1748. <https://doi.org/10.1016/j.bbmem.2017.04.019>.
- Järvinen, A., Heikkilä, P., Keskinen, J., Yli-Ojanperä, J., 2017. Particle charge-size distribution measurement using a differential mobility analyzer and an electrical low pressure impactor. *Aerosol Sci. Technol.* 51 (1), 20–29. <https://doi.org/10.1080/02786826.2016.1256469>.
- Jorba, O., Pérez, C., Roca-denbosch, F., Baldasano, J., 2004. Cluster analysis of 4-day back trajectories arriving in the Barcelona area, Spain, from 1997 to 2002. *J. Appl. Meteorol.* 43 (6), 887–901. [https://doi.org/10.1175/1520-0450\(2004\)043<0887:caodbt>2.0.co;2](https://doi.org/10.1175/1520-0450(2004)043<0887:caodbt>2.0.co;2).
- Kim, D., Chen, Z., Zhou, L.-F., Huang, S.-X., 2018. Air pollutants and early origins of respiratory diseases. *Chronic Dis. Transl. Med.* 4 (2), 75–94. <https://doi.org/10.1016/j.cdtm.2018.03.003>.
- Kalkstein, L.S., Tan, G., Skindlov, J.A., 2002. An evaluation of three clustering procedures for use in synoptic climatological classification. *J. Clim. Appl. Meteorol.* 26 (6), 717–730. [https://doi.org/10.1175/1520-0450\(1987\)026<0717:aeotcp>2.0.co;2](https://doi.org/10.1175/1520-0450(1987)026<0717:aeotcp>2.0.co;2).
- Kanamitsu, M., 2002. Description of the NMC global data assimilation and forecast system. *Weather Forecasting* 4 (3), 335–342. [https://doi.org/10.1175/1520-0434\(1989\)004<0335:dotngd>2.0.co;2](https://doi.org/10.1175/1520-0434(1989)004<0335:dotngd>2.0.co;2).
- Kassomenos, P.A., Gryparis, A., Katsouyanni, K., 2007. On the association between daily mortality and air mass types in Athens, Greece during winter and summer. *Int. J. Biometeorol.* 51 (4), 315–322. <https://doi.org/10.1007/s00484-006-0062-7>.
- Kerminen, V.-M., Chen, X., Vakkari, V., Petäjä, T., Kulmala, M., Bianchi, F., 2018. Atmospheric new particle formation and growth: review of field observations. *Environ. Res. Lett.* 13. <https://doi.org/10.1088/1748-9326/aadf3c> 103003.
- Kubicki, M., Odzimek, A., Neska, M., 2016. Relationship of ground-level aerosol concentration and atmospheric electric field at three observation sites in the Arctic, Antarctic and Europe. *Atmos. Res.* 178–179: 329–246. doi:10.1016/j.atmosres.2016.03.029.
- Kulmala, M., Petäjä, T., Ehn, M., Thornton, J., Sipilä, M., Worsnop, D.R., Kerminen, V. M., 2014. Chemistry of atmospheric nucleation: on the recent advances on precursor characterization and atmospheric cluster composition in connection with atmospheric new particle formation. *Annu. Rev. Phys. Chem.* 65, 21–37. <https://doi.org/10.1146/annurev-physchem-040412-110014>.
- Kumar, S., Prasad, S., Yadav, K.K., Shrivastava, M., Gupta, N., Nagar, S., Bach, Q.V., Kamyab, H., Khan, S.A., Yadav, S., Malav, L.C., 2019. Hazardous heavy metals contamination of vegetables and food chain: role of sustainable remediation approaches – a review. *Environ. Res.* 179, (Pt A). <https://doi.org/10.1016/j.envres.2019.108792> 108792.
- Lamb, H.H., 1972. British Isles weather types and a register of the daily sequence of circulation patterns. In *Geophys Mem* (Vol. 116). Her Majesty's stationery office.
- Lelieveld, J., Klingmüller, K., Pozzer, A., Pöschl, U., Fnais, M., Daiber, A., Münzel, T., 2019. Cardiovascular disease burden from ambient air pollution in Europe reassessed using novel hazard ratio functions. *Eur. Heart J.* 40 (20), 1590–1596. <https://doi.org/10.1093/eurheartj/ehz135>.
- Li, N., Georas, S., Alexis, N., Fritz, P., Xia, T., Williams, M.A., Horner, E., Nel, A., 2016. A work group report on ultrafine particles (American Academy of Allergy, Asthma & Immunology): why ambient ultrafine and engineered nanoparticles should receive special attention for possible adverse health outcomes in human subjects. *J. Allergy Clin. Immunol.* 138 (2), 386–396. <https://doi.org/10.1016/j.jaci.2016.02.023>.
- Marjamäki, M., Ntziachristos, L., Virtanen, A., Ristimäki, J., Keskinen, J., Moisio, M., Palonen, M. and Lappi, M., 2002. Electrical Filter Stage for the ELPI. SAE Technical Paper Series 2002-01-0055.
- Markou, M.T., Kassomenos, P., 2010. Cluster analysis of five years of back trajectories arriving in Athens, Greece. *Atmos. Res.* 98 (2–4), 438–457. <https://doi.org/10.1016/j.atmosres.2010.08.006>.
- Martin, D., Bergametti, G., Strauss, B., 1990. On the use of the synoptic vertical velocity in trajectory model: validation by geochemical tracers. *Atmos. Environ. Part A* 24 (8), 2059–2069. [https://doi.org/10.1016/0960-1686\(90\)90240-N](https://doi.org/10.1016/0960-1686(90)90240-N).
- McGregor, G.R., 1993. A multivariate approach to the evaluation of the climatic regions and climatic resources of China. *Geoforum* 24 (4), 357–380.
- Moody, J.L., Galloway, J.N., 1988. Quantifying the relationship between atmospheric transport and the chemical composition of precipitation on Bermuda. *Tellus B* 40 B (5), 463–479. <https://doi.org/10.1111/j.1600-0889.1988.tb00117.x>.
- Moody, J.L., Samson, P.J., 1989. The influence of atmospheric transport on precipitation chemistry at two sites in the midwestern United States. *Atmos. Environ.* (1967), 23(10), 2117–2132. doi:10.1016/0004-6981(89)90173-X.
- Philipp, A., 2009. Comparison of principal component and cluster analysis for classifying circulation pattern sequences for the European domain. *Theor. Appl. Climatol.* 96 (1–2), 31–41.
- Remoundaki, E., Papayannis, A., Kassomenos, P., Mantas, E., Kokkalis, P., Tsezos, M., 2013. Influence of saharan dust transport events on PM2.5 concentrations and composition over Athens. *Water Air Soil Pollut.* 224 (1), 1373. <https://doi.org/10.1007/s11270-012-1373-4>.
- Royé, D., Zarrabeitia, M.T., Fdez-Arroyabe, P., Álvarez Gutiérrez, A., Santurtún, A., 2018. Role of apparent temperature and air pollutants in hospital admissions for acute myocardial infarction in the North of Spain. *Rev. Esp. Cardiol.* <https://doi.org/10.1016/j.recesp.2018.05.032>.
- Sanderson, P., Delgado-Saborit, J.M., Harrison, R.M., 2014. A review of chemical and physical characterisation of atmospheric metallic nanoparticles. *Atmos. Environ.* 94, 353–365. <https://doi.org/10.1016/j.atmosenv.2014.05.023>.
- Santurtún, A., González-Hidalgo, J.C., Sánchez-Lorenzo, A., Zarrabeitia, M.T., 2015. Surface ozone concentration trends and its relationship with weather types in Spain (2001–2010). *Atmos. Environ.* 101, 10–22. <https://doi.org/10.1016/j.atmosenv.2014.11.005>.
- Santurtún, A., Rasilla, D.F., Riancho, L., Zarrabeitia, M.T., 2017. Relationship between chronic obstructive pulmonary disease and air pollutants depending on the origin and trajectory of air masses in the North of Spain. *Arch. Bronconeumol.* 53 (11), 616–621. <https://doi.org/10.1016/j.arbres.2017.03.017>.
- Sanyal, S., Rochereau, T., Maesano, C.N., Com-Ruelle, L., Annesi-Maesano, I., 2018. Long-term effect of outdoor air pollution on mortality and morbidity: a 12-year follow-up study for metropolitan France. *Int. J. Environ. Res. Public Health* 15 (11). <https://doi.org/10.3390/ijerph15112487>.
- Scientific Committee on Emerging and newly identified health risks (SCENIHR). (2006). The appropriateness of existing methodologies to assess the potential risks associated with engineered and adventitious products of nanotechnologies. Visited on 11th October 2019: https://ec.europa.eu/health/ph_risk/committees/04_scenihr/docs/scenihr_o_003b.pdf.
- Stohl, A., 1998. Computation, accuracy and applications of trajectories—a review and bibliography. *Atmos. Environ.* 32 (6), 947–966. [https://doi.org/10.1016/S1352-2310\(97\)00457-3](https://doi.org/10.1016/S1352-2310(97)00457-3).
- Yli-Ojanperä, J., Kannosto, J., Marjamäki, M., Keskinen, J., 2010. Improving the nanoparticle resolution of the ELPI. *Aerosol Air Qual. Res.* 10 (360–366), 2010.
- Zhiqiang, Q., Konstantin Siegmann, K., Keller, A., Matter, U., Scherrer, L., Siegmann, H.C., 2000. Nanoparticle air pollution in major cities and its origin. *Atmos. Environ.* 34, 443–451.
- Dekati ELPI+, 2019. From <https://www.dekati.com/products/elpi/> (accessed 2019-06-08)